CHEMISTRY OF MATERIALS

COMMUNICATION

pubs.acs.org/cm

Structure of Ferroelectric Silver Niobate $AgNbO_3$

Masatomo Yashima,*,† Shota Matsuyama,† Rikiya Sano,‡ Mitsuru Itoh,§ Kenji Tsuda,‡ and Desheng Fu⊥

†Department of Materials Science and Engineering, Interdisciplinary Graduate School of Science and Engineering, Tokyo Institute of Technology, Nagatsuta-cho 4259, Midori-ku, Yokohama, 226-8502, Japan;

‡Institute of Multidisciplinary Research for Advanced Materials, Tohoku University, Katahira 2-1-1, Aoba-ku, Sendai, 980-8577, Japan;

§Materials and Structures Laboratory, Tokyo Institute of Technology, Nagatsuta-cho 4259, Midori-ku, Yokohama, 226-8503, Japan;

⊥Division of Global Research Leaders, Shizuoka University, Johoku 3-5-1, Naka-ku, Hamamatsu, 432-8561, Japan

Supporting Information

KEYWORDS: $AgNbO_3$, silver niobate, crystal structure, ferroelectric, polarization, piezoelectric, neutron, synchrotron, diffraction, Rietveld, first principles

Ferroelectric materials with large spontaneous polarization and high dielectric and piezoelectric responses have a wide range of applications in various electronic devices such as, for examples, ferroelectric memories, capacitors, surface acoustic wave (SAW) devices, the transducers used in sonar, medical ultrasound tomography and new multipulse quieting fuel injectors in automobile. There exist two prototype ferroelectrics, $BaTiO_3$ and $PbTiO_3$. $BaTiO_3$ is generally used to fabricate the capacitive devices, but it remains issues of how to improve the temperature performance due to a structural transition around room temperature and its relatively low ferroelectric-paraelectric transition temperature T_c (∼120 °C). On the other hand, $PbTiO_3$-based compounds are widely used in piezoelectric devices because of their large piezoelectric responses. Their lead content, however, raises environmental concerns. Currently, increasing effort is being made to search novel lead-free materials.[1,2] Silver niobate ($AgNbO_3$) polycrystals were demonstrated to have an extremely large polarization of 52 μC cm^{-2} under an application of high electric field.[3] Chemical modification with Li or K substitution in the Ag site also leads to large polarization and piezoelectric responses in these solid solutions with high T_c (= 178−339 and 252 °C for Li and K substitutions, respectively).[4,5] Therefore, $AgNbO_3$ emerges as a promising mother-compound to develop the novel lead-free piezoelectrics as well as the microwave materials.[6] Moreover, $AgNbO_3$ is also a visible-light responsive photocatalyst, therefore, it is being explored to produce clean and recyclable hydrogen.[7]

In spite of its interesting properties and technological importance, there is a longstanding issue concerning its exact crystal structure at room temperature since the discovery of this compound in 1958.[8] Polarization or piezoelectric measurements indicate that $AgNbO_3$ is ferroelectric below T_c (∼67 °C).[3,8−10] In contrast, its crystal structure was refined by the centrosymmetric *Pbcm* space group,[11−13] which cannot allow the occurrence of ferroelectricity. Such a discrepancy is essential due to the complicated structure, which consists of both complex NbO_6 octahedral tilting and small atomic displacements, leading to the difficulty in determining its structure exactly. In the present work, we have unambiguously clarified the crystal structure of $AgNbO_3$ through comprehensive investigations by using convergent-beam electron diffraction, electron diffraction, the neutron and synchrotron powder diffraction, and first principles calculations. We show that $AgNbO_3$ is ferroelectric at room temperature and has a noncentrosymmetric orthorhombic $Pmc2_1$ space group. The atomic displacements are ordered in the ferrielectric way in the lattice, which is extremely rare in ferroelectric materials, resulting to a net spontaneous polarization along the *c*-axis in $Pmc2_1$. These results allow us to gain a deep insight into the physical and chemical properties of $AgNbO_3$, and also provide essential structural information for further theoretical calculations on its electronic structure, and future material design.[14]

$AgNbO_3$ polycrystals were prepared by a solid-state reaction method at 1050 °C for 6 h in O_2 atmosphere.[3] The chemical composition was confirmed by the Inductively Coupled Plasma (ICP) analysis. Neutron powder diffraction data of $AgNbO_3$ were measured at 23.0 °C using a 150 detector system HERMES[15] at a neutron wavelength of 1.82646 Å. Synchrotron powder diffraction measurements were carried out at 25.1 °C by a high-angular-resolution multidetector system[16] installed at the BL-4B$_2$ beamline of Photon Factory. Both neutron- and synchrotron-diffraction data were analyzed by Rietveld method using a computer program RIETAN-FP.[17] The structure was drawn by VESTA.[18] Unit-cell and atomic positions of $AgNbO_3$ were optimized based on the density functional theory (DFT) with a program vasp[19] (See the details in the Supporting Information, part A). Convergent-beam electron diffraction (CBED) and selected-area electron diffraction (SAED) experiments were performed at room temperature using an energy-filter transmission electron microscope of JEM-2010FEF operated at an accelerating voltage of 100 kV, for the determination of crystal point- and space-groups.[20]

CBED patterns were obtained from specimen areas of a few nm in diameter. Single domain areas free from lattice defects were carefully chosen. Figure S1a in Supporting Information B shows a CBED pattern taken at the [100] incidence. Zeroth-order Laue zone (ZOLZ) reflections are seen in the center of the

Received: November 26, 2010
Revised: January 18, 2011
Published: March 07, 2011

pattern, and higher-order Laue zone (HOLZ) reflections are seen as a ring in the outer part of the pattern. Some reflection disks surrounded by rectangles are magnified in the insets with different contrast. While a mirror symmetry perpendicular to the b^*-axis is found, no mirror symmetry perpendicular to the c^*-axis is seen, as is indicated by white arrowheads. CBED patterns taken at the [010] and [001] incidences showed m and $2mm$ symmetries, respectively. These results indicate that the point group is noncentrosymmetric $mm2$ and that the spontaneous polarization is along the c-direction.

Images b and c in Figure S1 in Supporting Information B show SAED patterns taken at the [010] and [001] incidences, respectively. The lattice type has been determined to be primitive P, because 100 and 010 reflections were observed.

In the HOLZ reflections of 1 0 11 and 1 0 $\bar{1}\bar{1}$ in Figure S1a in Supporting Information B, A-type dynamical extinction lines are seen as denoted by black arrowheads. A_2-type dynamical extinction line is also observed in the inset of the 005 reflection though it has very weak intensity. These show the existence of a c-glide symmetry in the (010) plane and a 2_1-screw axis along the b-axis.[20] Thus, the space group has been uniquely determined to be $Pmc2_1$ (No. 26). It is noted that the systematic absence of the reflections $h0l$ (l = odd) in the [010] SAED pattern of Figure S1b in Supporting Information B is consistent with the c-glide symmetry of the space group $Pmc2_1$.

Rietveld refinements of the neutron and synchrotron diffraction data of $AgNbO_3$ were successfully performed on the basis of a distorted perovskite-type structure with $Pmc2_1$ space-group symmetry (Table 1, and Figure S2 and Table S2 in the Supporting Information, part C and D). The weighted reliability (R) factor in the Rietveld analysis of neutron data, R_{wp} = 5.26% for $Pmc2_1$ model was better than that for $Pbcm$ one, R_{wp} = 5.43%. The R factors based on the Bragg intensity and structure factors were R_B = 1.65% and R_F = 0.82%, respectively, for the neutron data of $Pmc2_1$ $AgNbO_3$. The R factors for synchrotron data of $Pmc2_1$ $AgNbO_3$ were R_{wp} = 8.76%, R_B = 2.34% and R_F = 1.47%. The unit-cell parameters of $Pmc2_1$ $AgNbO_3$ were a = 15.64773(3) Å $\approx 4a_p$, b = 5.55199(1) Å $\approx (2)^{1/2}a_p$, and c = 5.60908(1) Å $\approx (2)^{1/2}a_p$, where a_p denotes the pseudocubic perovskite cell parameter. The $Pmc2_1$ model with $a \approx 2a_p$, which was reported for $NaNbO_3$,[21−23] was not appropriate for $AgNbO_3$, because (i) hkl reflections (h = odd numbers) based on the $a \approx 4a_p$ lattice were observed in electreon, neutron and synchrotron diffraction data and (ii) Rietveld fits based on the $Pmc2_1$ model with $a \approx 2a_p$ were much worse (R_{wp} = 18.17% for neutron, R_{wp} = 19.41% for synchrotron data) (Figures S1, S3 and S4 in the Supporting Information, part B and E).

It was found that $Pmc2_1$ $AgNbO_3$ has a perovskite-type structure consisting of corner-linked NbO_6 octahedron and Ag atoms (Figure 1a). The bond valence sums (BVSs) of Nb1 and Nb2 sites were estimated to be 4.8 and 4.9, respectively, which are consistent with the valence 5+ of Nb^{5+}. The BVSs of Ag1, Ag2, and Ag3 sites were estimated to be 1.0, 1.1 and 1.0, respectively, which are consistent with the valence 1+ of Ag^+. The refined unit-cell parameters and atomic positions from neutron data agree well with those from synchrotron data (See Table 1 and Table S2 in the Supporting Information, part D). The optimized structure of $Pmc2_1$ $AgNbO_3$ by first-principles DFT calculations also agree with the experimental data (see Table S1 in the Supporting Information, part A). These results indicate the validity of the present refined structure.

Table 1. Refined crystallographic parameters and reliability factors in Rietveld analysis of synchrotron-powder-diffraction data for $Pmc2_1$ $AgNbO_3$ taken at 25.1 °C.[a]

	fractional coordinate			
site	x	y	z	U (Å^2) [b]
Ag1 4c	0.7499(3)	0.7468(3)	0.2601(5)	0.0114(2)
Ag2 2b	1/2	0.7466(6)	0.2379(5)	= U(Ag1)
Ag3 2a	0	0.7424(4)	0.2759(6)	= U(Ag1)
Nb1 4c	0.6252(2)	0.7525(5)	0.7332(2)	0.00389(18)
Nb2 4c	0.1253(2)	0.24159	0.27981	= U(Nb1)
O1 4c	0.7521(9)	0.7035(12)	0.783(2)	0.0057(5)
O2 2b	1/2	0.804(3)	0.796(3)	= U(O1)
O3 4c	0.6057(7)	0.5191(18)	0.4943(18)	= U(O1)
O4 4c	0.6423(7)	0.0164(18)	0.539(2)	= U(O1)
O5 2a	0	0.191(3)	0.256(3)	= U(O1)
O6 4c	0.1339(9)	0.0410(17)	0.980(2)	= U(O1)
O7 4c	0.1154(8)	0.4573(17)	0.5514(19)	= U(O1)

[a] Orthorhombic space group $Pmc2_1$. Number of formula units of $AgNbO_3$ in a unit cell: Z = 8. Unit-cell parameters: a = 15.64773(3) Å, b = 5.55199(1) Å, c = 5.60908(1) Å, $\alpha = \beta = \gamma$ = 90 deg. Unit-cell volume: V = 487.2940(17) Å^3. Reliability factors in the Rietveld analysis: R_{wp} = 8.76%, R_p = 6.34%, R_e = 5.18%, R_{wp}/R_e = 1.69, R_B = 2.34%, R_F = 1.47%. Occupancy factor is fixed to be 1. [b] U(X): Isotropic atomic displacement parameter of X atom at the X site.

The NbO_6 octahedra show $(a_p^- b_p^- c_p^+)/(a_p^- b_p^- c_p^-)$ tilting (= $(a_p^- a_p^- c_p^+)/(a_p^- a_p^- c_p^-)$, because b_p^- is equivalent with a_p^-), where the tilt angles along $[0\,1\,\bar{1}]$ (= a_p), $[0\,\bar{1}\,\bar{1}]$ (= b_p) and [100] (= c_p) axes of $Pmc2_1$ $AgNbO_3$ were estimated to be 5.749−6.795, 5.749−6.795 and 7.014−7.016°, respectively (See the details in Figures S5−S8 in the Supporting Information, parts F−I). The AgO_{12} polyhedron volumes (50.5- 52.1 Å^3) are larger than those of NbO_6 octahedra (10.5−10.7 Å^3) (see Table S3 in the Supporting Information, part J). The Nb−O bond length was ranged from 1.86 to 2.16 Å, while the Ag−O distance had a larger distribution from 2.43 to 3.18 Å (see Table S4 in the Supporting Information, part K). The distortion index based on bond lengths[24] and quadratic elongation[25] of AgO_{12} polyhedron were larger than those of NbO_6 (Table S3 in the Supporting Information J). The distortions make the off-center displacements of Ag and Nb atoms in AgO_{12} and NbO_6 polyhedra, respectively (arrows in Figure 1a).

Although $AgNbO_3$ is ferroelectric below T_c (~67 °C),[3,8−10] the structure of $AgNbO_3$ has been refined by the centrosymmetric $Pbcm$ in the literature.[11−13] The invalid $Pbcm$ $AgNbO_3$ is antiferroelectic, because the Ag and Nb atoms exhibit antiparallel displacements along b axis, which forms the center of symmetry (arrows and crosses (+) in Figure 1b). Notable feature of $Pmc2_1$ $AgNbO_3$ is the atomic displacement along the c axis (Figure 1a). The Nb1 displacement is larger than the Nb2 one. The Ag2 and Ag3 displacements are not equaled. Ag1 atom has a displacement. Average displacement values were estimated to be 0.097(17), 0.04(2) and 0.072(17) Å for Ag, Nb and O atoms, respectively. The small value for Nb atoms is attributable to the nearly antiparallel displacements (Figure 1a). On the contrary, six Ag atoms shift in the [001] direction and two Ag atoms displace in the $[0\,0\,\bar{1}]$ direction. Total spontaneous polarization was estimated to be −3.7(3.5) μC cm^{-2} using the refined structure of $Pmc2_1$ $AgNbO_3$ from neutron data. Here the number

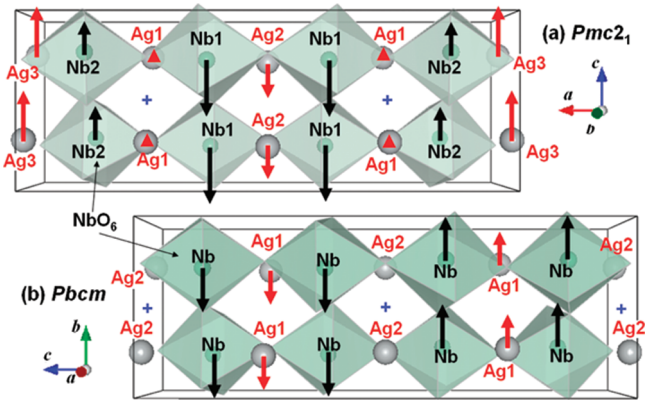

Figure 1. Refined crystal structures of $AgNbO_3$ from neutron powder diffraction data taken at 23 °C, by (a) $Pmc2_1$ and (b) *Pbcm* space groups. Green polyhedron stands for an NbO_6 octahedron. Gray and green spheres denote Ag and Nb atoms, respectively. Red and black arrows stand for the displacements of Ag^+ and Nb^{5+} ions, respectively, from the center of bonded oxygen positions. A cross (+) stands for the center of symmetry in the *Pbcm* structure.

in the parentheses is the estimated standard deviation. This value 3.7(3.5) μC cm^{-2} agrees with the values determined from the hysteresis loop under low electric fields (0.041 μC cm^{-2} for 11 kV cm^{-1} (ref 9), 0.095 μC cm^{-2} for 2.95 kV cm^{-1} (ref 10)) within the 3σ where σ (= 3.5 μC cm^{-2}) is the estimated standard deviation. Contributions of Ag^+, Nb^{5+} and O^{2-} ions to the total spontaneous polarization were 2.5, 5.3, and −11.5 μC cm^{-2}, respectively.

$AgNbO_3$ exhibits a sharp maximum in the permittivity−temperature curve at T_c (∼ 67 °C).[3,8,9] The spontaneous polarization of $AgNbO_3$ decreases with an increase of temperature and becomes zero at T_c, which indicates the ferroelectric-paraelectric M_1-M_2 phase transition.[9] Around the T_c, no structural phase transition in $AgNbO_3$ has been detected in the previous diffraction studies.[8,12,13,26] The present work strongly suggests that the M_1-M_2 transition at T_c (∼67 °C) is a $Pmc2_1$−*Pbcm* transformation, which is induced by the atomic displacements along the *c* axis (Figure 1).

In conclusion, we have successfully addressed the longstanding issue on the crystal structure of ferroelectric $AgNbO_3$. CBED measurements on a single domain region of $AgNbO_3$ allow us to unambiguously identify its space group to non-centrosymmetric $Pmc2_1$. The neutron and synchrotron powder diffraction analyses, and first-principles DFT calculations allow us to reliably determine the atomic positions in the unit cell. The net spontaneous polarization in $AgNbO_3$ is essentially due to the atomic displacements along the *c* axis in $Pmc2_1$. The ferroelectric-paraelectric transition ($T_c \approx$ 67 °C) is also suggested to be a $Pmc2_1$−*Pbcm* transformation. Our findings will be favored for the understanding of the physical and chemical properties of $AgNbO_3$ and for the design of $AgNbO_3$-based piezoelectric materials and photocatalysts.

■ ASSOCIATED CONTENT

Ⓢ Supporting Information. Crystallographic information (CIF); additional tables and figures (PDF). This material is available free of charge via the Internet at http://pubs.acs.org/.

■ ACKNOWLEDGMENT

We thank Prof. K. Ohoyama, Prof. T. Ida, and Mr. M. Ohkawara for arranging the neutron- and synchrotron-diffraction experiments. We thank also to Dr. T. Wakita for the ICP analysis. This research work was partially supported by a Grant-in-Aid for Scientific Research (B) (21360318, 20340070, and 22340078) from the Ministry of Education, Culture, Sports, Science and Technology of Japan. This work was carried out under the Joint-use Research Programs for Neutron Scattering, Institute for Solid State Physics (ISSP), the University of Tokyo, at the Research Reactor JRR-3, JAEA (Proposal 8768) and Photon Factory of KEK (Proposal 2006G263).

■ REFERENCES

(1) Saito, Y.; Takao, H.; Tani, T.; Nonoyama, T.; Takatori, K.; Homma, T.; Nagaya, T.; Nakamura, M. *Nature* **2004**, *432*, 84–87.
(2) Rödel, J.; Jo, W.; Seifert, K. T. P.; Anton, E.-M.; Granzow, T.; Damjanovic, D. *J. Am. Ceram. Soc.* **2009**, *92*, 1153–1177.
(3) Fu, D.; Endo, M.; Taniguchi, H.; Taniyama, T.; Itoh, M. *Appl. Phys. Lett.* **2007**, *90*, 252907–1−3.
(4) Fu, D.; Endo, M.; Taniguchi, H.; Taniyama, T.; Koshihara, S.; Itoh, M. *Appl. Phys. Lett.* **2008**, *92*, 172905–1−3.
(5) Fu, D.; Itoh, M.; Koshihara, S. J. *Appl. Phys.* **2009**, *106*, 104104–1−6.
(6) Valant, M.; Suvorov, D. *J. Am. Ceram. Soc.* **1999**, *82*, 88–93.
(7) Kato, H.; Kobayashi, H.; Kudo, A. *J. Phys. Chem. B* **2002**, *106*, 12441–12447.
(8) Francombe, M. H.; Lewis, B. *Acta Crystallogr.* **1958**, *11*, 175–178.
(9) Kania, A.; Roleder, K.; Lukaszewski, M. *Ferroelectrics* **1984**, *52*, 265–269.
(10) Saito, A.; Uraki, S.; Kakemoto, H.; Tsurumi, T.; Wada, S. *Mater. Sci. Eng., B* **2005**, *120*, 166–169.
(11) Fabry, J.; Zikmund, Z.; Kania, A.; Petricek, V. *Acta Crystallogr., Sect. C* **2000**, *56*, 916–918.
(12) Sciau, Ph; Kania, A.; Dkhil, B.; Suard, E.; Ratuszna, A. *J. Phys.: Condens. Matter* **2004**, *16*, 2795–2810.
(13) Levin, I.; Krayzman, V.; Woicik, J. C.; Karapetrova, J.; Proffen, T.; Tucker, M. G.; Reaney, I. M. *Phys. Rev. B* **2009**, *79*, 104113–1−14.
(14) Yashima, M. *J. Ceram. Soc. Jpn.* **2009**, *117*, 1055–1059.
(15) Ohoyama, K.; Kanouchi, T.; Nemoto, K.; Ohashi, M.; Kajitani, T.; Yamaguchi, Y. *Jpn. J. Appl. Phys. Part 1* **1998**, *37*, 3319–3326.
(16) Toraya, H.; Hibino, H.; Ohsumi, K. *J. Synchrotron Radiat.* **1996**, *3*, 75–84.
(17) Izumi, F.; Momma, K. *Solid State Phenom.* **2007**, *130*, 15–20.
(18) Momma, K.; Izumi, F. *J. Appl. Crystallogr.* **2008**, *41*, 653–658.
(19) Kresse, G.; Joubert, D. *Phys. Rev. B* **1999**, *59*, 1758–1775.
(20) Tanaka, M. *International Tables for Crystallography*, 3rd ed.; Shumueli, U., Ed.; International Union of Crystallography; Springer: Dordrecht, The Netherlands, 2008; Vol. B, pp 307−356.
(21) Shuvaeva, V. A.; Antipin, M. Y.; Lindeman, S. V.; Fesenko, O. E.; Smotakov, V. G.; Struchkov, Y. T. *Sov. Phys. Crystallogr.* **1992**, *37*, 814–817.
(22) Shanker, V.; Samal, S. L.; Pradhan, G. K.; Narayana, C.; Ganguli, A. K. *Solid State Sci.* **2009**, *11*, 562–569.
(23) Johnston, K. E.; Tang, C. C.; Parker, J. E.; Kneight, K. S.; Lightfoot, P.; Ashbrook, S. E. *J. Am. Chem. Soc.* **2010**, *132*, 8732–8746.
(24) Baur, W. H. *Acta Crystallogr., Sect. B* **1974**, *30*, 1195–1215.
(25) Robinson, K.; Gibbs, G. V.; Ribbe, P. H. *Science* **1971**, *172*, 567–570.
(26) Pawelczyk, M. *Phase Transitions* **1987**, *8*, 273–292.